Indian Journal of Experimental Biology
Vol. 64, November 2026, pp. 1008-1018
DOI: 10.56042/ijeb.v64i11.25267

Evaluating the Cytotoxic and Pro-apoptotic effects of Artemisinin on Human breast cancer cell lines *via* MTT, Caspase assays, and Gene expression studies

Parismita Borah[1], Mousumi Dutta[1], Asifa Banu[2], Utpal Nath[3], Neelanjana Sarmah[1], Aktarul Islam Siddique[1], Kongkana Goswami[3], Aniruddha Jakharia[1] & Biswajyoti Borkakoty[1]*

[1]Regional VRDL, ICMR-Regional Medical Research Centre, N.E. Region, Dibrugarh-786 001, Assam, India
[2]Department of Microbiology, School of Lifesciences, Bharathidasan University, Tiruchirappalli-620 024, Tamil Nadu, India
[3]Department of Medical Laboratory Technology, The Assam Kaziranga University, Jorhat-785 006, Assam, India

Received 09 December 2025; revised 09 September 2026

Artemisinin, a sesquiterpene lactone derived from *Artemisia annua*, has demonstrated promising anti-cancer properties. This study aimed to evaluate the compound's pro-apoptotic and cytotoxic potential in MCF-7 human breast cancer cells. MCF-7 cells were treated with varying concentrations of Artemisinin (0.78–100 µg/mL), and apoptosis was assessed by measuring caspase-3, -8, and -9 activities at 24, 48, and 72 h post-treatment. Cell viability and cytotoxicity were quantified using the MTT assay, and IC_{50} values were calculated accordingly. Gene expression of BAX and BCL-2 was analyzed *via* qPCR using the ΔΔCt method. Two-way ANOVA was performed to assess the combined effects of Artemisinin concentration and exposure time. A consistent dose- and time-dependent increase in caspase activity was noted, with Caspase-9 showing the most marked elevation at 72 h, indicating strong activation of the intrinsic pathway. Artemisinin treatment significantly reduced MCF-7 cell viability, particularly at 24 and 48 h. IC_{50} values were 0.84 µg/mL (24 h), 1.33 µg/mL (48 h), and 2.82 µg/mL (72 h), demonstrating a time-dependent reduction in sensitivity. Two-way ANOVA showed significant effects of both Artemisinin concentration and exposure time on viability and cytotoxicity, with a notable interaction for cytotoxicity ($p = 0.0268$). BAX expression was upregulated, while BCL-2 was downregulated in a concentration and time dependent manner. Artemisinin induces significant cytotoxicity and apoptosis in MCF-7 breast cancer cells through caspase activation and modulation of BAX/BCL-2 expression, supporting its potential as a promising anti-cancer therapeutic agent.

Keywords: Artemisinin, BAX gene, BCL-2, Breast cancer, Caspase, MCF-7, MTT assay.

Cancer remains one of the leading global health challenges, accounting for nearly 10 million deaths in 2020 alone[1]. Among the most prevalent malignancies, breast cancer is the most diagnosed cancer worldwide[2]. The increasing incidence, aggressive nature, and frequent development of resistance to standard therapies in both breast and liver cancers underscore the urgent need for novel, effective and safer treatment alternatives.

Conventional chemotherapeutic agents often exhibit non-specific toxicity, leading to damage of normal cells and severe side effects. Furthermore, resistance to standard therapies in triple-negative breast cancer (TNBC) and advanced-stage HCC poses substantial therapeutic challenges[3]. This has intensified research interest in plant-derived compounds with anticancer potential, particularly those that exhibit selectivity toward cancer cells while sparing normal tissues.

One such compound is artemisinin, a sesquiterpene lactone originally isolated from *Artemisia annua*, which has revolutionized malaria treatment. Over the past two decades, artemisinin and its semi-synthetic derivatives (*e.g.*, artesunate, dihydroartemisinin) have demonstrated broad-spectrum anticancer activity across various cell lines and tumor types, including breast and liver cancers[4]. The antitumor properties of artemisinin are primarily attributed to its endoperoxide bridge, which generates reactive oxygen species (ROS) in the presence of intracellular iron, leading to oxidative stress, DNA damage, and ultimately apoptosis[5]. Breast cancer cells are known to exhibit high iron uptake due to increased expression of transferrin receptors, making them particularly susceptible to artemisinin-induced oxidative damage[6]. Despite these promising features, a comprehensive understanding of artemisinin's cytotoxic effects and underlying molecular mechanisms across different cancer types remains to be fully elucidated. Breast cancer cells often reprogram iron metabolism to support rapid proliferation and metastasis, commonly

*Correspondence:
E-mail: biswaborkakoty@gmail.com

showing upregulated transferrin receptor 1 (TfR1) and intracellular iron accumulation[7]. This iron-rich phenotype creates biochemical vulnerability: artemisinin and its semi-synthetic derivatives are activated by ferrous iron (or iron-containing adducts) to generate carbon-centered radicals and reactive oxygen species (ROS), thereby producing iron-dependent oxidative damage in tumor cells[8]. Multiple mechanistic studies and reviews indicate that artemisinin exerts anticancer activity through a constellation of processes including ROS-mediated DNA damage, apoptosis and non-apoptotic death pathways (notably ferroptosis), modulation of autophagy, and interference with cell-cycle and survival signaling[9]. Preclinical work also shows that exploiting transferrin conjugates or iron-loading strategies can enhance artemisinin selectivity and cytotoxicity against cancer cells, supporting the therapeutic rationale for targeting iron metabolism together with artemisinin-based compounds[10].

Despite these promising mechanistic and preclinical data, the breadth and context-dependence of artemisinin's cytotoxic effects remain incompletely defined: different cancer types and subtypes vary in iron handling, antioxidant defences (*e.g.*, GPX4, ferritin), and molecular drivers that determine susceptibility to ferroptosis or ROS-driven apoptosis, and clinical translation has thus far been limited to a few early-phase trials[4]. Therefore, a detailed, comparative assessment of artemisinin's molecular actions across cancer lineages integrating iron metabolism status, ROS responses, and cell-death pathway engagement is needed to guide rational combination strategies and biomarker development for clinical testing.

To accurately assess the therapeutic potential of artemisinin, a multi-parametric approach is essential. Cytotoxicity assays, such as the 3-(4, 5-dimethylthiazol-2-yl)-2,5-diphenyl tetrazolium bromide (MTT) assay, are widely used to measure cell viability and metabolic activity following drug treatment. These assays provide a baseline understanding of a compound's antiproliferative capacity. Prior studies have confirmed artemisinin's dose- and time-dependent inhibition of cancer cell proliferation in breast (MCF-7). The MTT assay is widely used due to its reliability and sensitivity in screening drug effects on various cancer cell lines[11]. In the context of artemisinin treatment, MTT assays have revealed dose- and time-dependent reductions in cell viability across several cancer types, including breast and liver cancer[12].

In addition to cytotoxicity evaluation, understanding the biochemical pathways activated during artemisinin-induced cell death is crucial. Apoptosis, or programmed cell death, is a tightly regulated cellular process that is often disrupted in cancer. Caspases, a family of cysteine proteases, play a central role in executing apoptosis by cleaving specific substrates and orchestrating cellular disassembly. Artemisinin has been shown to activate both intrinsic (mitochondrial-mediated) and extrinsic (death receptor-mediated) apoptotic pathways, often marked by increased expression and activity of initiator caspases (such as caspase 8 and 9) and effector caspases (such as caspase 3)[13]. Caspase activity assays are therefore a critical component of any study aimed at elucidating artemisinin's pro-apoptotic effects. Artemisinin has been shown to activate both intrinsic (mitochondrial) and extrinsic (death receptor-mediated) apoptotic pathways by stimulating key caspases such as caspase 3, 8 and 9[14].

In parallel, gene expression profiling provides vital insights into the regulatory pathways affected by drug treatment. Real-time PCR and related molecular techniques allow for the quantification of gene transcripts involved in apoptosis (*e.g.*, BAX, BCL-2), oxidative stress (*e.g.*, Nrf2, HO-1), and cell cycle regulation (*e.g.*, p21, cyclin D1). Notably, artemisinin has been shown to upregulate pro-apoptotic genes and downregulate anti-apoptotic or proliferative genes, thereby promoting programmed cell death and inhibiting tumor progression[15]. Previous studies have demonstrated that artemisinin treatment modulates several of these key gene networks, suggesting a multifaceted mode of action[16]. In breast cancer cells, artemisinin has been reported to downregulate BCL-2 while upregulating pro-apoptotic genes like BAX, leading to mitochondrial membrane permeabilization and cell death. Similarly, artemisinin and its derivatives have been reported to modulate signaling pathways involved in tumor progression, including the Wnt/β-catenin pathway and PI3K/Akt pathways[17-18].

These pathways control cell survival, proliferation, and resistance to therapy, suggesting that artemisinin may offer a multi-targeted approach to cancer treatment. Artemisinin has emerged as a promising anticancer agent capable of inhibiting breast cancer cell proliferation through apoptosis induction, caspase activation, modulation of Bax/Bcl-2 gene expression, and regulation of key signaling pathways involved in tumor progression and survival[19]. Artemisinin and its derivatives, originally developed as potent antimalarial agents, have recently gained considerable attention for their broad-spectrum anticancer properties, including the induction of oxidative stress, cell-cycle

arrest, apoptosis, and inhibition of angiogenesis in various human cancer models[20]. Artemisinin-loaded PLGA nanofibers have demonstrated enhanced cytotoxic activity against SK-BR-3 breast cancer cells by increasing intracellular ROS generation and modulating key apoptotic markers, including Bax, Bcl-2, caspase-3, and p53**,** compared with free artemisinin [21]. Artemisinin and its derivatives, characterized by their unique endoperoxide bridge, have emerged as promising anticancer agents, with accumulating evidence demonstrating their ability to inhibit tumor growth through multiple molecular mechanisms, supporting their potential application in cancer therapy[22].

In this context, the present study aims to comprehensively investigate the anticancer effects of artemisinin on MCF-7 cell lines by integrating cytotoxicity (MTT assay), biochemical (caspase activity), and molecular (gene expression) analyses. By correlating changes in cell viability with apoptotic enzyme activation and gene expression alterations, this study intends to delineate the mechanistic pathways through which artemisinin exerts its effects. The findings may contribute to the growing body of evidence supporting the repurposing of artemisinin as a potential adjunct or alternative therapy in the management of breast and liver cancers.

Materials and Methods

Cell culture

MCF-7 cells were sourced from the American Type Culture Collection (ATCC, USA). Cryopreserved stocks were revived and cultured under sterile conditions in Roswell Park Memorial Institute (RPMI)-1640 medium (Gibco, USA) supplemented with 10% fetal bovine serum (FBS) and 1% antibiotic-antimycotic (Sigma-Aldrich, USA). Cultures were maintained in a humidified incubator at 37°C with 5% CO_2. The medium was replenished every 48 h to sustain optimal viability. Upon reaching 70–80% confluence, cells were sub-cultured at a 1:3 ratio using 1X trypsin-EDTA. Morphological assessment was performed using an inverted microscope to monitor cell health and adherence throughout the culture period.

Seeding of cells

Cells at ~90% confluence were gently washed twice with 1X PBS and treated with 1% trypsin-EDTA (HiMedia, India) to facilitate detachment. After 5-6 min of incubation at 37°C, the cell detachment was verified microscopically. The enzymatic activity was neutralized by adding complete medium, and the cell suspension was triturated to achieve a single-cell suspension. This was centrifuged at 1000 rpm for 10 min, and the pellet was resuspended in fresh medium. Cell viability and density were determined using a hemocytometer. For MTT and caspase assays, 10,000 cells/well were seeded in 96-well plates, while 50,000 cells/well were used for gene expression studies in 24-well plates. Plates were incubated for 48 h at 37°C in 5% CO_2 before treatment.

Preparation of Artemisinin drug

Artemisinin (Merck, Germany) was initially dissolved in dimethyl sulfoxide (DMSO) to prepare a 1 mg/mL stock solution. This stock was serially diluted using complete growth medium (RPMI-1640 with 10% FBS) to obtain working concentrations of 100, 50, 25, 12.5, 6.25, 3.12, 1.56, and 0.78 µg/mL. All working solutions were freshly prepared before use. The final DMSO concentration in treated wells was maintained below 0.1% to eliminate solvent-induced cytotoxicity. Solutions were protected from light and used within the same experimental session to ensure drug stability.

Treatment of cells

Cells in 96-well plates were treated with the prepared artemisinin concentrations in triplicate after 48 h of seeding. Blank wells (medium only) and untreated control wells (with medium and DMSO vehicle) were included in triplicate for background correction/normalization in the ΔΔCt method. Treatment durations were set at 24, 48, and 72 h to capture time-dependent effects. For each assay endpoint (MTT, caspase, and gene expression), separate plates were used. Morphological observations were recorded before and after treatment using an inverted microscope. All treatments were repeated independently at least twice to ensure reproducibility.

Preparation of Cell lysate for Caspase assay

Following incubation, treated wells were washed with 4°C pre-cooled PBS to remove residual media. Cells were detached with 10 µL of 1X trypsin-EDTA, followed by neutralization with 200 µL of complete medium. Suspended cells were transferred to 1.5 mL tubes and centrifuged at 1000 rpm for 10 min. The resulting pellet was washed with pre-cooled PBS and resuspended in 200 µL PBS. Cells were lysed using an ultrasonicator for 5 min on ice. Lysates were centrifuged at 15,000 rpm for 10 min at 2–8°C to separate cell debris. The supernatant

containing soluble protein was collected and stored for caspase assay analysis.

Caspase assay

The activity of caspase-3, -8, and -9 was quantified using ELISA kits (Elabscience, China) specific for each isoform. Cell lysates from treated and control groups were processed according to the manufacturer's instructions. Briefly, standards and samples were added to pre-coated ELISA plates, followed by incubation with enzyme conjugates and substrate solutions. After color development, absorbance was read at 450 nm using a microplate reader. Increased caspase activity in treated samples compared to controls was interpreted as evidence of apoptosis induction. All samples were processed in triplicate to ensure accuracy and reproducibility.

MTT assay

To assess cell viability post-treatment, an MTT assay was performed. After artemisinin exposure, 10 µL of MTT reagent (Merck, Germany) was added to each well, and the plates were incubated for 4 h at 37°C. Formazan crystals formed were dissolved using 100 µL of isopropanol containing 0.04 N HCl. Absorbance was measured immediately at 570 nm using an ELISA plate reader. The percentage of viable cells was calculated relative to untreated controls, DMSO vehicle, and IC_{50} values were derived using dose-response curves. Morphological alterations were recorded microscopically to support biochemical results.

Gene expression analysis

After treatment, cells were detached using 1X trypsin-EDTA and neutralized with complete medium. Cell suspensions were centrifuged at 1000 rpm for 10 min. The pellet was washed and resuspended in medium and processed for nucleic acid extraction. RNA integrity was verified before proceeding to reverse transcription. Cells were either processed immediately or stored at -80°C until RNA extraction. All steps were performed using RNase-free reagents and conditions to preserve nucleic acid quality for downstream qPCR.

Nucleic acid extraction

Genomic DNA was isolated using the QIAamp DNA Mini Kit (Qiagen, Germany) following the manufacturer's protocol. Cells were lysed in ATL buffer and digested with Proteinase K at 56°C for 30 min. The lysate was further processed with AL buffer and ethanol before being applied to a silica-based spin column. Wash steps were performed with AW1 and AW2 buffers, and DNA was eluted in 70 µL of AE buffer. The concentration and purity were evaluated using spectrophotometry. DNA samples were stored at –20°C for short-term or –80°C for long-term use.

Two-Step RT-qPCR for gene expression

For cDNA synthesis, 8.5 µL of Elution Primer Fragment 3HC mix (EPH3HC, Illumina) was combined with 8.5 µL of extracted sample. The mixture was gently mixed and incubated at 65°C for 3 min before holding at 4°C. First-strand cDNA synthesis was initiated by adding 8 µL of a master mix containing First Strand Mix HT and Reverse Transcriptase HT (Illumina), bringing the total volume to 25 µL. The thermal profile was: 25°C for 5 min, 50°C for 30 min, 80°C for 5 min, and hold at 4°C.

qPCR for BCL-2 and BAX gene expression

qPCR was conducted using SYBR Green-based detection to quantify BCL-2 and BAX expression. Reactions (20 µL) were prepared using 2× SYBR Green Fast qPCR Mix (ABclonal), 0.2 µM primers, and cDNA template. The cycling conditions included an initial denaturation at 95°C for 3 min, followed by 39 cycles of 95°C for 5 sec and 62°C for 34 sec. A melt curve analysis was performed to verify amplicon specificity. GAPDH was used as the internal control. Each sample was run in triplicate. Relative expression levels were calculated using the $2^{-}\Delta\Delta Ct$ method.

Statistical analysis

Statistical analysis was performed using SPSS version 26.0 (IBM Corp., Armonk, NY, USA). Two-way ANOVA was conducted to evaluate the effects of drug concentration and exposure time on cell viability and cytotoxicity. Normality and homogeneity of variances were assessed to meet ANOVA assumptions. Where appropriate, post-hoc comparisons were conducted using Tukey's HSD test. Graphs were generated using GraphPad Prism trial version (GraphPad Software, USA) or Microsoft Excel (Microsoft Corp., Redmond, WA, USA).

Results

Effect of Artemisinin on apoptotic markers and cell viability in MCF-7 Cells

The effect of Artemisinin on apoptosis induction in MCF-7 breast cancer cells was evaluated using

caspase 3, 8, and 9 assays at 24, 48, and 72 h post-treatment. The optical density (OD) values increased in a dose- and time-dependent manner across all three caspase assays, indicating progressive activation of apoptotic pathways.

In the Caspase-3 assay, the OD values showed a notable rise at higher Artemisinin concentrations, particularly at 100 µg/mL, where the OD reached 0.251 at 72 h, compared to the control (0.07) (Suppl. Table 1). A similar trend was observed for Caspase-9, with the OD peaking at 0.289 (72 h, 100 µg/mL), suggesting a strong activation of the intrinsic (mitochondrial) apoptosis pathway. Supplementary Table 2 represents the optical density of the Caspase-9 assay of MCF-7 cells treated with Artemisinin. Caspase-8, associated with the extrinsic pathway, also showed increased OD values, though comparatively moderate (maximum OD of 0.108 at 100 µg/mL, 72 h), implying its role but possibly less dominant than caspase-9 (Suppl. Table 3).

These results indicate that Artemisinin triggers apoptosis *via* both intrinsic and extrinsic pathways, with caspase-9 being more prominently activated, aligning with mitochondrial-mediated apoptosis mechanisms. The comparison of Caspase activity of MCF-7 cells treated with different concentration of the Artemisinin drug at various time periods is depicted in (Fig. 1).

Artemisinin induces dose- and time-dependent cytotoxicity in MCF-7 cells: MTT assay and IC_{50} analysis

The cytotoxic effect of Artemisinin on MCF-7 breast cancer cells was evaluated using the MTT assay at 24, 48, and 72 h post-treatment across a concentration gradient (0.78–100 µg/mL). The percentage of cell viability and cytotoxicity was calculated based on corrected optical density (OD) readings at 570 nm, relative to untreated controls (Table 1). A consistent decline in cell viability was observed with increasing drug concentrations, demonstrating a clear dose-dependent cytotoxic effect (Fig. 2)

At 24 h, cell viability significantly declined with increasing Artemisinin concentrations, with viability dropping to 40.11% at 25 µg/mL and 43.85% at 100 µg/mL (Fig. 3). The IC_{50} at this time point was calculated as 0.84µg/mL, indicating high potency of Artemisinin in short-term exposure (Table 4).

At 48 h, the cytotoxic effect was more pronounced, particularly at the highest concentration (100 µg/mL), where viability was reduced to 42.5%. The IC_{50} value increased slightly to 1.33 µg/mL, reflecting a moderate reduction in sensitivity over time.

Interestingly, at 72 h, a non-linear pattern in viability was observed. While some concentrations (*e.g.*, 1.56 and 3.12 µg/mL) showed relatively high viability (94.58% and 89.58%, respectively), the highest concentration (100 µg/mL) still produced substantial cytotoxicity (viability reduced to 53.75%). The IC_{50} value at 72 h was calculated as 2.82µg/mL, suggesting a reduced cytotoxic response upon prolonged exposure, possibly due to cell recovery mechanisms or drug instability over time.

To statistically validate these findings, a two-way ANOVA was performed. For cell viability, both drug concentration (46.51% variation, $p = < 0.0001$) and exposure time (21.73%, $p = < 0.0001$) had significant effects, while the interaction effect was not statistically significant ($p = 0.0977$). In contrast, for cytotoxicity, a significant interaction between concentration and time was found ($p = 0.0268$), along with strong independent effects of exposure time

Table 1 — Optical Density (OD) of MTT Assay at 570nm of MCF-7 cells treated with Artemisinin at 24, 48 and 72 h

Drug	Replicate 1	Replicate 2	Replicate 3	Mean OD	Corrected OD	Cell Visibility (%)	Cytotoxicity (%)
Concentration (µg/ ml)	24 48 72 Hr Hr Hr	24 48 72 Hr Hr Hr	24 48 72 Hr Hr Hr	24 48 72 Hr Hr Hr	24 48 72 Hr Hr Hr	24 48 72 Hr Hr Hr	24 48 72 Hr Hr Hr
Control	0.64 0.79 0.89	0.63 0.99 0.78	0.76 0.87 0.91	0.68 0.88 0.86	0.62 0.82 0.8	100 100 100	0 0 0
0.78	0.45 0.61 0.6	0.59 0.64 0.67	0.46 0.49 0.6	0.5 0.58 0.62	0.45 0.52 0.56	71.66 63.5 70.42	28.34 36.5 29.58
1.56	0.39 0.59 0.88	0.38 0.64 0.91	0.38 0.49 0.66	0.38 0.58 0.82	0.33 0.52 0.76	52.94 62.9 94.58	47.06 37.1 5.42
3.12	0.34 0.54 0.74	0.35 0.5 0.85	0.37 0.48 0.74	0.35 0.51 0.78	0.3 0.45 0.72	48.13 54.5 89.58	51.87 45.5 10.42
6.25	0.3 0.5 0.8	0.34 0.59 0.74	0.32 0.48 0.65	0.32 0.52 0.73	0.27 0.47 0.67	42.78 56.7 83.75	57.22 43.3 16.25
12.5	0.36 0.46 0.45	0.28 0.55 0.61	0.4 0.46 0.78	0.35 0.49 0.61	0.29 0.43 0.55	47.06 52.4 69.17	52.94 47.6 30.83
25	0.28 0.47 0.5	0.32 0.46 0.57	0.31 0.44 0.74	0.3 0.46 0.6	0.25 0.4 0.54	40.11 48.4 67.92	59.89 51.6 32.08
50	035 0.58 0.69	0.34 0.31 0.68	0.32 0.47 0.43	0.34 0.46 0.6	0.28 0.4 0.54	45.45 48.4 67.5	54.55 51.6 325
100	0.34 0.34 0.5	0.33 0.42 0.58	0.31 0.46 0.37	0.33 0.41 0.49	0.27 0.35 0.43	43.85 42.5 53.75	56.15 57.5 46.25
Blank	0.05 0.06 0.06	0.06 0.06 0.06	0.05 0.06 0.06	0.05 0.06 0.06			

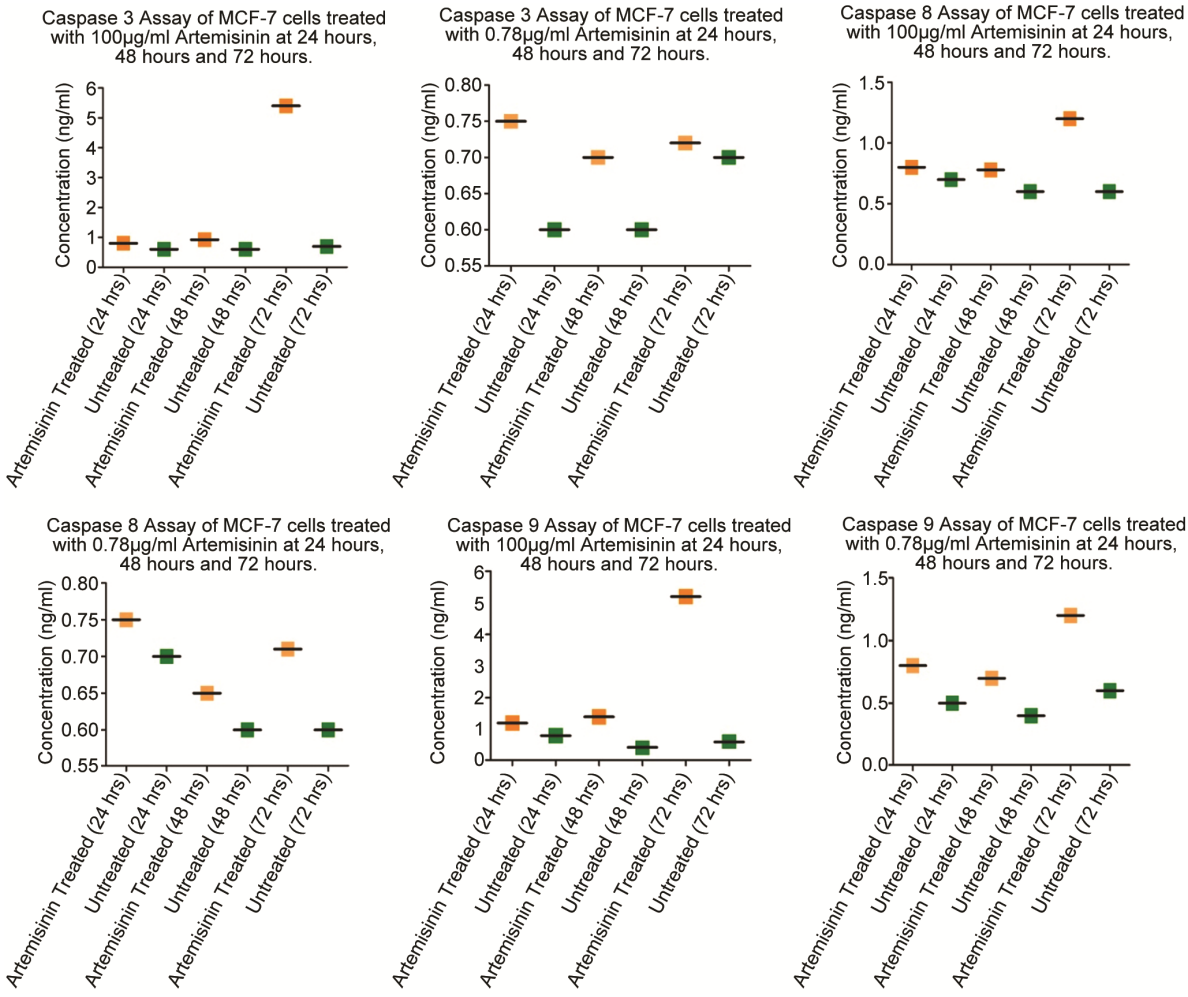


Fig. 1 — Caspase 3, 8 and 9 Assay of MCF-7 cells treated with 0.78 µg/mL and 100 µg/mL Artemisinin drug at 24 h, 48 h and 72 h

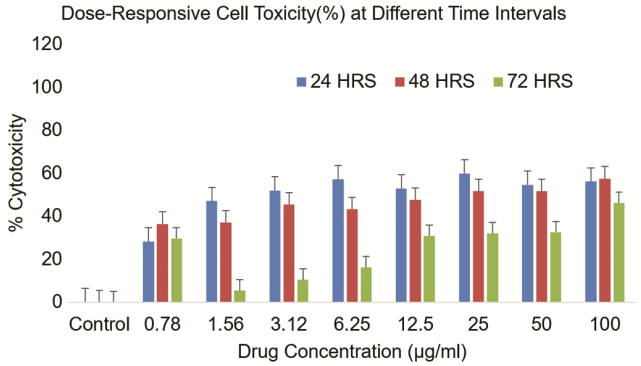


Fig. 2 — Comparison of Cytotoxicity (%) of MCF-7 cells treated with 0.78, 1.5, 3.12, 6.25, 12.5, 25, 50 and 100 µg/mL concentration of Artemisinin at 24, 48 and 72

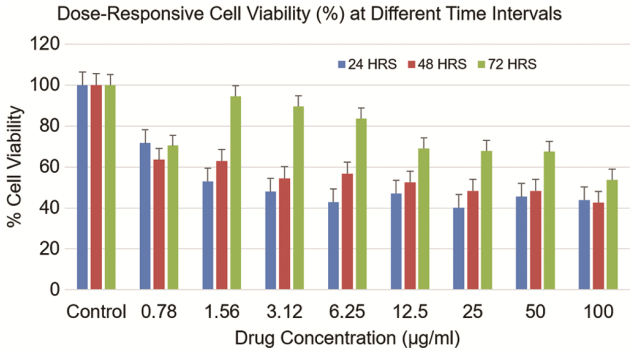


Fig. 3 — Comparison of Viability (%) of MCF-7 cells treated with 0.78, 1.5, 3.12, 6.25, 12.5, 25, 50 and 100 µg/mL concentration of Artemisinin at 24, 48 and 72 h

(56.23%, $p = < 0.0001$) and concentration (16.17%, $p = < 0.0001$).

Together, these results confirm that Artemisinin induces statistically significant, dose- and time-dependent cytotoxicity in MCF-7 cells. The trend of increasing IC_{50} over time suggests a potential adaptive response in cells or reduced bioavailability of the drug with extended exposure. These observations highlight the therapeutic potential of Artemisinin, especially for short-duration treatments, and emphasize the importance of optimizing dosing regimens in anticancer therapy.

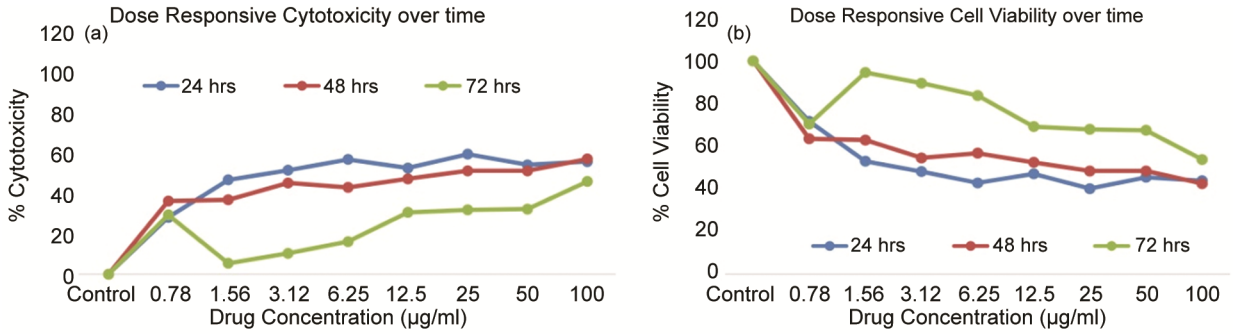


Fig. 4 — (a) Trend of Cytotoxicity (%) of Artemisinin treated MCF-7 cells at 24, 48 and 72 h, respectively; and (b) Trend of Cell Viability (%) of Artemisinin treated MCF-7 cells at 24, 48 and 72 h, respectively

Gene expression analysis of Pro- and Anti-apoptotic markers BAX and BCL-2 in Artemisinin-treated MCF-7 cells

The relative expression of the pro-apoptotic gene BAX and the anti-apoptotic gene BCL-2 was evaluated in MCF-7 cells treated with varying concentrations of Artemisinin (0.78–100 µg/mL) over 24, 48, and 72 h using the ΔΔCt method (Fig. 4). GAPDH was used as an internal reference gene, and untreated MCF-7 cells served as the control group for baseline comparison. Fold change values were calculated to determine the modulation in gene expression following drug treatment.

At 24 h, BAX expression showed a dose-dependent increase, with the most notable upregulation at lower concentrations (3.12 µg/mL, 2.11-fold; 1.56 µg/mL, 3.04-fold; and 0.78 µg/mL, 2.16-fold). In contrast, BCL-2 expression was downregulated in a dose-dependent manner, especially at higher concentrations (50 µg/mL, 0.41-fold; 100 µg/mL, 0.48-fold), indicating early apoptotic induction. Interestingly, at the lowest concentrations (1.56 µg/mL and 0.78 µg/mL), a paradoxical BCL-2 upregulation (6.79 and 7.21-fold, respectively) was observed, potentially indicating cellular stress response or survival signaling at sub-cytotoxic levels.

By 48 h, a marked upregulation of BAX was observed at all concentrations up to 25 µg/mL, with the highest expression at 100 µg/mL (2.97-fold). However, fold changes declined at lower concentrations (3.12 µg/mL and below), suggesting time-dependent modulation. BCL-2 expression during this period showed variable changes, with significant upregulation at 0.78 µg/mL (2.34-fold) and a moderate increase at intermediate doses (25–6.25 µg/mL and 1.5–1.7-fold), suggesting delayed anti-apoptotic responses in certain conditions.

After 72 h, BAX expression remained moderately upregulated across higher doses (1.48-fold at 50 µg/mL and 1.38-fold at 100 µg/mL) but showed a declining trend at lower concentrations. BCL-2 expression followed a reverse trend, showing gradual downregulation with decreasing concentration, reaching a minimum fold change of 0.53 at 0.78 µg/mL. This reciprocal pattern of BAX upregulation and BCL-2 downregulation over time and concentration reinforces Artemisinin's pro-apoptotic effect in MCF-7 cells (Suppl. Fig. 1).

Overall, the expression dynamics indicate that Artemisinin exerts its apoptotic effects in MCF-7 cells through upregulation of BAX and suppression of BCL-2, particularly in a dose- and time-dependent manner. The maximal pro-apoptotic shift was observed between 24–48 h of treatment, supporting its potential as an effective therapeutic agent in breast cancer treatment. Studies on different Artemisinin drug treatments during the period of 2015 to 2025 are depicted in (Suppl. Table 4) for reference.

Discussion

The current study comprehensively evaluates the anti-cancer potential of Artemisinin in human breast cancer (MCF-7) cells by examining its impact on apoptosis induction, cell viability, and apoptotic gene expression over 24, 48, and 72 h of treatment. The findings underscore Artemisinin's diverse mechanism of cytotoxic action, highlighting its therapeutic promise in breast cancer management.

Caspases are central to programmed cell death, with caspase-9 and caspase-3 being key mediators of the intrinsic mitochondrial pathway, while caspase-8 is associated with the extrinsic death receptor pathway. The significant, time- and dose-dependent increase in OD values in caspase-3, -8, and -9 assays observed in this study suggests that Artemisinin

triggers both apoptotic pathways, with predominant activation of the intrinsic pathway as evidenced by higher caspase-9 activity. The strong activation of caspase-9, particularly at 100 µg/mL after 72 h, supports mitochondrial involvement, consistent with previous reports where Artemisinin and its derivatives induced apoptosis *via* cytochrome c release and subsequent caspase-9 activation in various cancer models, including breast cancer[23-24]. Activation of caspase-8 further implies that Artemisinin may also engage the death receptor-mediated pathway, potentially amplifying downstream caspase-3 activation[10]. Previous studies demonstrated that dihydroartemisinin and artemisinin-transferrin conjugates can initiate reactive oxygen species (ROS) production, triggering mitochondrial depolarization and caspase cascades[25]. Together, these results corroborate that artemisinin induces apoptosis through ROS-dependent, mitochondria-mediated mechanisms, with cross-talk between intrinsic and extrinsic pathways enhancing cytotoxicity in cancer cells.

Caspase-3, the executioner caspase, also showed significant activation, suggesting downstream engagement following mitochondrial signalling. Moderate activation of caspase-8, while less prominent, indicates that Artemisinin may also partially act *via* death receptor-mediated pathways. This dual activation has been previously noted in Artemisinin-treated leukaemia and hepatocellular carcinoma cells[26]. The significant activation of caspase-3 observed in this study confirms the execution of apoptosis through downstream signalling, predominantly following mitochondrial perturbation. Moderate activation of caspase-8 suggests that artemisinin may also engage extrinsic, death receptor–mediated pathways [27]. Similar dual activation has been documented in artemisinin-treated breast, prostate, and lung cancer cells, highlighting its ability to trigger both intrinsic and extrinsic apoptotic routes [8,23]. Collectively, these findings reinforce the notion that artemisinin promotes apoptosis *via* multiple molecular mechanisms, offering a promising multitargeted strategy for cancer therapy.

MTT assay results demonstrated a clear dose-dependent decrease in MCF-7 cell viability upon ART treatment, affirming its cytotoxic potential. The IC_{50} values of 0.84 µg/mL (24 h), 1.33 µg/mL (48 h), and 2.82 µg/mL (72 h) suggest high initial sensitivity, which gradually reduces over time. This increase in IC_{50} could be attributed to cell adaptation mechanisms, possible degradation of Artemisinin (as artemisinin is unstable in aqueous solution over prolonged incubation), or induction of cellular defence mechanisms such as drug efflux pumps or stress response proteins[23,28]. Additionally, cancer cells can activate defence mechanisms, including upregulation of drug efflux transporters and antioxidant enzymes, thereby lowering ART sensitivity[29].

Interestingly, a non-linear pattern in viability at 72 h where lower ART doses showed relatively high viability may reflect hormetic effects, a phenomenon where low-dose exposures activate adaptive survival responses[30]. The significant interaction between drug concentration and exposure time for cytotoxicity, as revealed by two-way ANOVA ($p = 0.0268$), supports the complexity of ART's time-dependent cytotoxic behaviour. This underlines the importance of optimizing ART dosing schedules for maximizing anti-cancer efficacy while minimizing resistance or toxicity. The non-linear viability pattern at 72 h, where low artemisinin (ART) doses maintained higher cell survival, suggests a hormetic response, an adaptive mechanism in which mild stress induces cytoprotective pathways[26]. Such biphasic dose responses have been observed in cancer cells treated with oxidative stress-inducing agents, including ART derivatives[31]. The significant interaction between ART concentration and exposure time indicates complex time-dependent cytotoxic behaviour, possibly linked to metabolic adaptation and stress signaling [24,32]. Optimizing ART dosing schedules is therefore critical for maximizing efficacy while minimizing adaptive resistance.

Quantitative PCR analysis revealed that Artemisinin treatment significantly altered the expression of BAX (pro-apoptotic) and BCL-2 (anti-apoptotic) genes, supporting its role in mitochondrial pathway activation. At 24 h, low doses of Artemisinin (0.78–3.12 µg/mL) upregulated BAX expression (up to 3-fold), while higher doses significantly suppressed BCL-2 expression (*e.g.*, 0.41-fold at 50 µg/mL), indicating an early shift toward apoptosis. This aligns with reports that ART promotes oxidative stress and mitochondrial dysfunction, leading to BAX translocation and BCL-2 inhibition[33].

The paradoxical upregulation of BCL-2 at low Artemisinin concentrations at 24 h may represent a transient pro-survival response, potentially *via* activation of stress response transcription factors such

as NF-κB, which is known to induce BCL-2 expression under sub-lethal oxidative conditions[34]. However, by 48 h, a clearer apoptotic shift was evident: BAX expression peaked, especially at higher Artemisinin doses (up to ~3-fold), while BCL-2 showed variable responses, possibly reflecting the dynamic balance of pro and anti-apoptotic signals during prolonged exposure.

At 72 h, BAX remained moderately upregulated while BCL-2 showed marked downregulation at lower ART concentrations, confirming sustained pro-apoptotic pressure. The reciprocal regulation of these two genes highlights the role of Artemisinin in modulating mitochondrial apoptosis, consistent with previous studies showing Artemisinin-induced BAX activation and BCL-2 suppression in breast and ovarian cancer cells [35].

Artemisinin's ability to simultaneously modulate key apoptotic regulators, activate caspases, and reduce cell viability underscores its promise as an anticancer agent, particularly in estrogen receptor-positive breast cancer like MCF-7. Compared to standard chemotherapeutics such as paclitaxel, ART offers the advantage of selective toxicity toward cancer cells, with minimal impact on normal cells, as noted in multiple *in vitro* and in vivo models[24]. Its potential synergy with existing chemotherapeutics and its derivatization for enhanced bioavailability further enhance its clinical prospects.

Although apoptosis was the principal cell-death mechanism investigated in the present study, recent evidence indicates that artemisinin-induced cytotoxicity may also involve ferroptosis. A recent 2026 systematic review of artemisinin and its derivatives identified iron-dependent ROS accumulation, lipid peroxidation, and GPX4 inhibition as important mechanisms associated with ferroptotic cell death across several cancer models, including breast cancer [36]. Importantly, a recent study of dihydro artemisinin in triple-negative breast cancer demonstrated direct targeting and degradation of GPX4 through an autophagy-dependent mechanism, resulting in enhanced ferroptosis and reduced radioresistance[37]. These findings suggest that oxidative stress and iron-dependent mechanisms may also interact with apoptotic signaling during artemisinin-mediated cancer-cell death. However, because ferroptosis-related markers were not assessed in the present study, this mechanism remains a hypothesis requiring further direct experimental validation.

However, limitations such as the observed increase in IC_{50} over prolonged exposure and partial BCL-2 upregulation at sub-lethal doses warrant caution. These findings suggest the need for combination therapy strategies or sequential drug regimens to overcome potential resistance mechanisms. Moreover, additional studies using in vivo models and clinical samples are essential to validate the mechanistic findings and optimize therapeutic knowledge.

Conclusion

This study provides compelling evidence that Artemisinin induces apoptosis in MCF-7 breast cancer cells, primarily through activation of the intrinsic (mitochondrial) pathway and to a lesser extent the extrinsic pathway, as reflected by caspase activation profiles. It downregulates anti-apoptotic BCL-2, upregulates pro-apoptotic BAX, and reduces cell viability in a dose- and time-dependent manner. However, the observed apoptotic and cytotoxic responses occur predominantly at higher concentrations, which may exceed achievable therapeutic levels in clinical settings. This highlights a key limitation for its standalone use as an anticancer agent. Nonetheless, these findings underscore the potential of developing more potent Artemisinin analogues or derivatives with enhanced efficacy at lower doses. Furthermore, the integration of Artemisinin into rationally designed combination therapies could synergize its apoptotic effects, reduce the required dose, and mitigate resistance, paving the way for optimized cancer treatment strategies. Interestingly, a non-linear pattern in viability at 72 h where lower ART doses showed relatively high viability may reflect hormetic effects, a phenomenon where low-dose exposures activate adaptive survival responses.

Acknowledgement

This study was funded by the Indian Council of Medical Research, Government of India. Project Sanction Order Number: 5/13/61/2020/NCD-III Dated: 26.03.2021. (Parismita Borah), (Mousumi Dutta), (Asifa Banu) and (Utpal Nath) performed the experiments. (Parismita Borah), (Mousumi Dutta), (Neelanjana Sarmah) and (Aktarul Islam Siddique) analysed the data. (Parismita Borah), (Mousumi Dutta) wrote the manuscript. (Aniruddha Jakharia) & (Biswajyoti Borkakoty) reviewed the manuscript. (Biswajyoti Borkakoty) designed the experiment.

Conflict of interest

All authors declare no conflict of interest.

References

1 Sung H, Ferlay J, Siegel RL, Laversanne M, Soerjomataram I, Jemal A & Bray F, Global cancer statistics 2020: GLOBOCAN estimates of incidence and mortality worldwide for 36 cancers in 185 countries. *CA Cancer J Clin*, 71 (2021) 209.

2 Siegel RL, Miller KD, Fuchs HE & Jemal A, Cancer statistics, 2024. *CA Cancer J Clin*, 74 (2024) 12.

3 So JY, Oh J, Lipkowitz S & Yang L, Triple negative breast cancer (TNBC): Non-genetic tumor heterogeneity and immune microenvironment: Emerging treatment options. *Pharmacol Ther*, 237 (2022) 108253.

4 Wen L, Chan BC, Qiu MH, Leung PC & Wong CK, Artemisinin and its derivatives as potential anticancer agents. *Molecules*, 29 (2024) 3886.

5 Zhou X, Suo F, Haslinger K & Quax WJ, Artemisinin-type drugs in tumor cell death: Mechanisms, combination treatment with biologics and nanoparticle delivery. *Pharmaceutics*, 14 (2022) 395.

6 Zhou X, Soto-Gamez A, Nijdam F, Setroikromo R & Quax WJ, Dihydroartemisinin-transferrin adducts enhance TRAIL-induced apoptosis in triple-negative breast cancer in a p53-independent and ROS-dependent manner. *Front Oncol*, 11 (2022) 789336.

7 Shen Y, Li X, Dong D, Zhang B, Xue Y & Shang P, Transferrin receptor 1 in cancer: A new sight for cancer therapy. *Am J Cancer Res*, 8 (2018) 916.

8 Nakase I, Lai H, Singh NP, Sasaki T & Richardson DR, Transferrin receptor-dependent cytotoxicity of artemisinin-transferrin conjugates on cancer cells. *Bioorg Med Chem Lett*, 19 (2009) 5046.

9 Xu C, Zhang H & Zhou W, Artemisinins as anticancer drugs: Novel therapeutic approaches and mechanisms. *Front Pharmacol*, 11 (2020) 529.

10 Zhou X, Soto-Gamez A, Nijdam F, Setroikromo R & Quax WJ, Dihydroartemisinin-transferrin adducts enhance TRAIL-induced apoptosis in triple-negative breast cancer in a p53-independent and ROS-dependent manner. *Biomed Pharmacother*, 151 (2022) 113145.

11 Stockert JC, Blázquez-Castro A, Cañete M, Horobin RW & Villanueva A, MTT assay for cell viability: Intracellular localization of the formazan product is in lipid droplets. *Acta Histochem*, 114 (2012) 785.

12 Kumari K, Keshari S, Sengupta D, Sabat SC & Mishra SK, Transcriptome analysis of genes associated with breast cancer cell motility in response to Artemisinin treatment. *BMC Cancer*, 17 (2017) 858.

13 Hou J, Wang D, Zhang R & Wang H, Experimental therapy of hepatoma with artemisinin and its derivatives: *In vitro* and *in vivo* activity, chemosensitization, and mechanisms of action. *Clin Cancer Res*, 14 (2008) 5519.

14 Hamacher-Brady A, Stein HA, Turschner S, Toegel I, Mora R, Jennewein N, Efferth T, Eils R & Brady NR, Artesunate activates mitochondrial apoptosis in breast cancer cells *via* iron-catalyzed lysosomal reactive oxygen species production. *J Biol Chem*, 286 (2011) 6587.

15 Crespo-Ortiz MP & Wei MQ, Antitumor activity of artemisinin and its derivatives: From a well-known antimalarial agent to a potential anticancer drug. *Biomed Res Int*, 2012 (2012) 247597.

16 Wong YK, Xu C, Kalesh KA, He Y, Lin Q, Wong WSF, Shen HM & Wang J, Artemisinin as an anticancer drug: Recent advances in target profiling and mechanisms of action. *Med Res Rev*, 37 (2017) 1492.

17 Tong Y, Liu Y, Zheng H, Zheng L, Liu W, Wu J, Ou R, Zhang G, Li F, Hu M, Liu Z & Lu L, Artemisinin and its derivatives can significantly inhibit lung tumorigenesis and tumor metastasis through Wnt/β-catenin signaling. *Oncotarget*, 7 (2016) 31413.

18 Wu R, Gao Y, Wu J, Wang C & Yang L, Semi-synthetic product dihydroartemisinin inhibited fibronectin-1 and integrin-β1 and interfered with the migration of HCCLM6 cells *via* PI3K-AKT pathway. *Biotechnol Lett*, 42 (2020) 917.

19 Yildirim MA, Sevinc B, Paydas S, Karaselek MA, Duran T, Kuccukturk S, Vatansev H, Cetiz MV, Caprioli G, Acquaticci L, Cakilcioglu U & Zengin G, Exploring the anticancer potential of Dianthus orientalis in pancreatic cancer: A molecular and cellular study. *Food Biosci*, 66 (2025) 106183.

20 Xia Y, Shi C, Lu J, Zhu Z, Li M, Pan Y, Huang X, Zhang L & Liu A, Artemisinin and its derivatives from molecular mechanisms to clinical applications: New horizons beyond antimalarials. *Int J Mol Sci*, 26 (2025) 8409.

21 Eslami Vaghar M, Dadashpour M & Derakhshan E, Artemisinin-loaded mesoporous silica nanoparticles/ electrospun poly(lactic-co-glycolic acid) composite nanofibers for enhanced anticancer efficiency in breast cancer cells. *Cancer Nanotechnol*, 15 (2024) 58.

22 Wen L, Chan BC, Qiu MH, Leung PC & Wong CK, Artemisinin and its derivatives as potential anticancer agents. *Molecules*, 29 (2024) 3886.

23 Jamalzadeh L, Ghafoori H, Aghamaali M & Sariri R, Induction of apoptosis in human breast cancer MCF-7 cells by a semi-synthetic derivative of artemisinin: A caspase-related mechanism. *Iran J Biotechnol*, 15 (2017) 157.

24 Crespo-Ortiz MP & Wei MQ, Antitumor activity of artemisinin and its derivatives: From a well-known antimalarial agent to a potential anticancer drug. *J Biomed Biotechnol*, 2012 (2012) 247597.

25 Nakase I, Gallis B, Takatani-Nakase T, Oh S, Lacoste E, Singh NP, Goodlett DR, Tanaka S, Futaki S, Lai H & Sasaki T, Transferrin receptor-dependent cytotoxicity of artemisinin-transferrin conjugates on prostate cancer cells and induction of apoptosis. *Cancer Lett*, 274 (2009) 290.

26 Wong YK, Xu C, Kalesh KA, He Y, Lin Q, Wong WSF, Shen HM & Wang J, Artemisinin as an anticancer drug: Recent advances in target profiling and mechanisms of action. *Med Res Rev*, 37 (2017) 1492.

27 Lakhani SA, Masud A, Kuida K, Porter GA Jr, Booth CJ, Mehal WZ, Inayat I & Flavell RA, Caspases 3 and 7: Key mediators of mitochondrial events of apoptosis. *Science*, 311 (2006) 847.

28 Beekman AC, Woerdenbag HJ, Van Uden W, Pras N, Konings AW & Wikström HV, Stability of artemisinin in aqueous environments: Impact on its cytotoxic action to Ehrlich ascites tumour cells. *J Pharm Pharmacol*, 49 (1997) 1254.

29 Calabrese EJ, Baldwin LA & Tuthill RW, Hormesis: A highly generalizable and reproducible phenomenon with important implications for risk assessment. *Risk Anal*, 19 (1999) 261.
30 Calabrese EJ & Mattson MP, How does hormesis impact biology, toxicology, and medicine? *NPJ Aging Mech Dis*, 3 (2017) 13.
31 Efferth T, Dunstan H, Sauerbrey A, Miyachi H & Chitambar CR, The anti-malarial artesunate is also active against cancer. *Int J Oncol*, 18 (2001) 767.
32 Efferth T, Molecular pharmacology and pharmacogenomics of artemisinin and its derivatives in cancer cells. *Curr Drug Targets*, 7 (2006) 407.
33 Karin M & Lin A, NF-κB at the crossroads of life and death. *Nat Immunol*, 3 (2002) 221.
34 Prasad S, Ravindran J & Aggarwal BB, NF-kappaB and cancer: How intimate is this relationship? *Mol Cell Biochem*, 336 (2010) 25.
35 Mao H, Gu H, Qu X, Sun J, Song B, Gao W, Liu J & Shao Q, Involvement of the mitochondrial pathway and Bim/Bcl-2 balance in dihydroartemisinin-induced apoptosis in human breast cancer *in vitro*. *Int J Mol Med*, 31 (2013) 213.
36 Dag SRO, Tatli IIT & Ozkan AMG, The role of artemisinin and its derivatives in cancer therapy *via* ferroptosis: A systematic review of *in vitro*, in vivo, and in silico studies. *Anticancer Agents Med Chem*, 26 (2026) 1127.
37 Wu Y, Chen D, Wang X, Song M, Wu J, Wu S & Liao K, Dihydroartemisinin targets GPX4 to induce autophagy-dependent ferroptosis and reduce radioresistance in triple-negative breast cancer. *Free Radic Biol Med*, 246 (2026) 35.